Applied and Computational Mechanics 10 (2016) 17–26

Applied and Computational Mechanics

Design of the blisk of an aircraft turbojet engine and verification of its resonance free operation

L. Chromek[a,*]

[a] *První brněnská strojírna Velká Bíteš, a. s., Vlkovská 279, 595 12 Velká Bíteš, Czech Republic*

Received 11 February 2016; received in revised form 20 May 2016

Abstract

Integral turbine wheels belong to one of the most stressed parts of jet aircraft engines. In addition to high rotational speeds and temperatures, they are also subjected to dynamic forces from a non-uniform pressure field in the flow path. Dynamic forces even at a relatively small amplitude can cause failure by fatigue, which leads to fracture of blades and crash of the machine. These adverse conditions, called resonance, should be avoided already in the design stage when a suitable choice of stator vanes and the number of blades can move the critical speed of the blisk beyond the operating speed or at least reduce their influence. In the case of a small jet engine produced by the První brněnská strojírna (PBS) Velká Bíteš, the operating speed is of nearly half of the entire speed range of the machine. This makes the design of a proposed turbine wheel very complicated. A higher harmonic order of aerodynamic excitation is almost always present, its influence was therefore tested experimentally by vibration tests in the test station PBS Velká Bíteš.

Keywords: jet engine, blisk, critical speed, experimental modal analysis, resonance

1. Introduction

After a series of accidents of older blisks at testing stations, it was decided that a new geometry of blisk and inlet guide vanes will be created at the Aerospace Technology Division PBS Velká Bíteš, which would be resonance-free in the operating speed range. This condition necessitated new approaches in the design of the dynamic properties of blisk and their subsequent testing methodology.

The turbine aircraft engine works in a very wide range of operating speeds, which makes its application, not only in terms of dynamics, very complicated. By changing the geometry of the turbine's blade or disk, the natural frequency usually changes only slightly, and thus, it is more appropriate to change the excitation from the whole blade row. Aerodynamic excitation arises naturally from all around the circumference spaced obstacles in the flow path. The effect of stator vanes is, however, the largest due to their distance from the blisk, and therefore, this article will focus mainly on this effect.

Blisks operate at high rotational speeds and temperatures, which have a significant influence on their natural frequency and thus the critical speed. Influence of temperature and rotational speed are included to the calculation of the modal characteristics. Experimental verification is always more evident. Since the excitation from the pressure field is not ideally harmonic, higher harmonic orders of the excitation are generated. In this case, their influence is investigated experimentally.

*Corresponding author. Tel.: +420 566 822 957, e-mail: chromek.l@pbsvb.cz.

2. Numerical analysis of modal properties

One of the first and very important steps in the development of a new blisk of aircraft turbojet engine is to specify the modal properties—in this case, the natural frequencies and modal shapes. On this basis, the critical speed is found which must be avoided during operation or must be quickly overcome. Flexible integral disks have very low damping, which is not considered in the calculations.

First four natural frequencies are found using the finite element method (FEM) implemented in software ANSYS Workbench. According to the experience of the operation, the most dangerous are especially the first four mode shapes of the blade. Displacement and stress level of modal shapes of blades are normalised by the mass matrix.

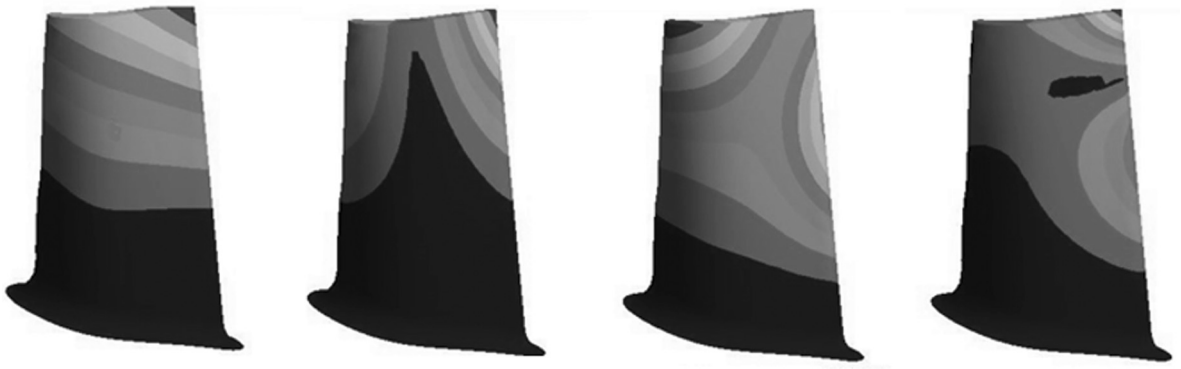

Fig. 1. First four modal shapes (displacement)

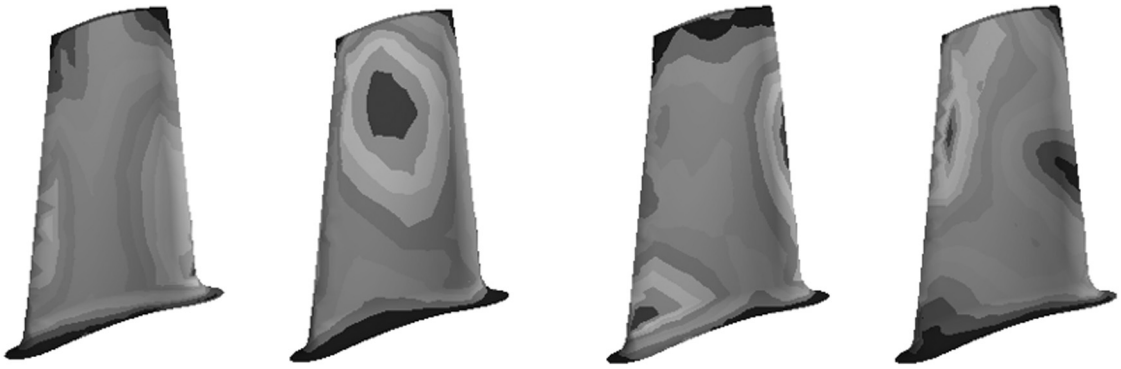

Fig. 2. Von Misses stress of the first four modal shapes

In an iterative procedure and in conjunction with the CFD Department at PBS Velká Bíteš, a design of the blades was proposed with the objective to locate the first natural frequency over four times the rotational speed representing the backward traveling wave (stationary in space) excited from non-uniform pressure field. The largest possible difference was also requested to be between the first and second natural frequencies.

For a more accurate solution, it was necessary to consider the influence of rotational speed and temperature in the calculation of the modal properties phase. With increasing rotational speed, the disc and blades have to be reinforced (stiffened) and their natural frequency increases. This relation is described by the following form [8]

$$f_n = \sqrt{f_0^2 + \left(\frac{n}{n_{\max}}\right)^2 (f_{\max}^2 - f_0^2)}, \tag{1}$$

where f_n is natural frequency at rotational speed n, f_0 is natural frequency at zero rotational speed, $f_{\max}$ is natural frequency at rotational speed $n_{\max}$. Furthermore, with increasing temperature, the natural frequencies decrease. Therefore, the temperature effect was included into the analysis of the natural frequencies. The operating temperature of the blisk is in the range from 427 to 871 °C. To describe the effect of temperature, the following analytical relation was used [8]:

$$f_T = f_{20} \cdot \varphi = f_{20} \cdot \sqrt{\frac{E_T}{E_{20}}}, \tag{2}$$

where f_T is natural frequency of the blisk at temperature T, E_T is Young's modulus at temperature T and E_{20} is Young's modulus at 20 °C. The above analytical relationships were confirmed by numerical calculations of modal properties with pre-stress and thermo-elastic analysis in ANSYS. The Campbell diagram (for 13 nodal diameters, will be explained in the following section) with the aforementioned effects is shown in Fig.3. The first order of nozzle pass frequency (NPF) is equal to 13$^{\text{th}}$ engine order (EO), the second order of NPF is equal to 26$^{\text{th}}$ EO and so on.

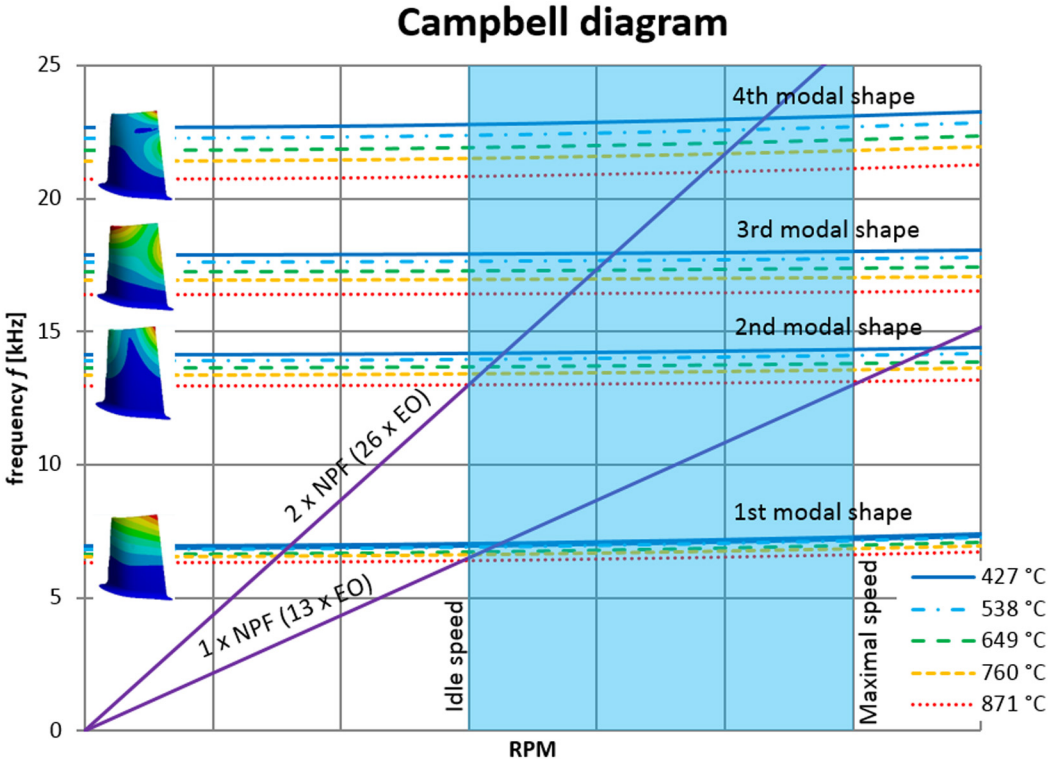

Fig. 3. Campbell diagram with the effect of temperature and centrifugal force

3. Coupled modal shapes of the blisk

Blisks can generally vibrate by different modal shapes, however, only the bending modes with nodal diameters are of any practical significance in aircrafts blisks. Not all modal shapes of blisk vibration can be really excited. To identify excitable modal shapes with the number k of nodal diameters, the following general equation was used

$$k_{c,h} = |c \cdot r - h \cdot s| = \begin{cases} \dfrac{r}{2} & \text{for even } r, \\ \dfrac{1}{2}(r-1) & \text{for odd } r. \end{cases} \tag{3}$$

The formula was originally published by Kushner in 1980 [3]. Its validity was verified during testing of impeller in VZLÚ [2] and on the basis of failure analysis of the operation and testing of impellers with covering disc carried out by Kushner [5].

Excitable modal shapes were computed for $1 \div 3$ harmonic order h of aerodynamic excitation and $0 \div 3$ rotating shapes of excitation c. The constant c is an integer, usually close to the s/r ratio, where s is the number of stator vanes and r is the number of periodical structures (blades). Probably, only the basic vectors of excitation, which belong to the first three numbers of c, which are nearest to the s/r ratio, [1,4,7], will have any practical significance. For the excitation from the non-uniform pressure field caused by the 13 stator vanes, the ratio value becomes close to 0. The next closest integer of c include 1 and 2.

The number of vanes was, therefore, selected so that the first harmonic order of the first rotating vector of excitation represented by the straight lines in Campbell diagram (Fig. 3) has not an intersection with any natural frequencies in operating range. These conditions are met by the stator with 13 vanes because of space between the first and second natural frequencies. Table 1 contains the excitable modal shapes of blisk with k nodal diameters obtained by equation (4). The wakes behind the stator vanes are considered as the excitation source. Excitable shapes are highlighted.

Table 1. Excitable modes combination of $s = 13$ vanes, $r = 37$ periodical structures, c rotating shape of excitation and h harmonic order

$k_{c,h}$	h		
c	1	2	3
0	**13**	26	39
1	24	**11**	2
2	61	48	35

According to Table 1, the blisk will be excited by "zero" rotating vector of excitation, thus the backward wave has a zero angular speed, the same as the vector of operating excitation. In this case of 13 nodal diameters, the waves standing in space will be formed.

From a practical point of view, a significant vector is the first rotating vector of excitation, where $c = 1$. Since the intensity of the higher harmonics of the interaction excitation of relatively dense stator rows decreases rapidly, it usually suffices to consider only $h = 1$ and 2. When the number of nodal diameters is greater than 18 (according to equation (4)), each blade vibrates individually, i.e., without nodal diameters. Because of the number of rotor blades and stator vanes, no travelling wave will be formed.

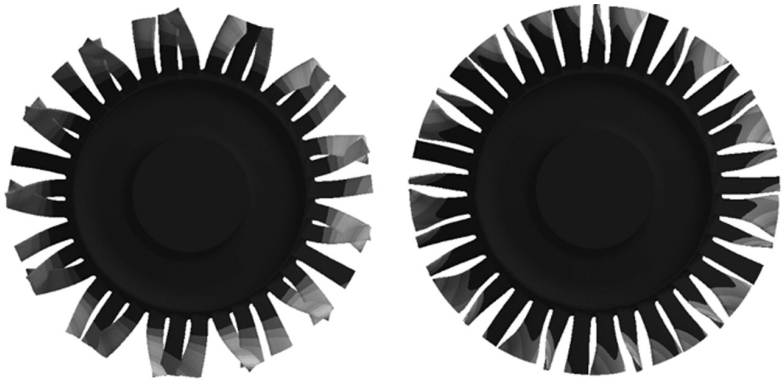

Fig. 4. Coupled vibration of the blisk (total displacement): (*left*) 1st modal shape with 13 nodal diameters, (*right*) 2nd modal shape with 13 nodal diameters

In the case of the second harmonic order of excitation vector, the blisk will vibrate with 11 nodal diameters in form of travelling waves.

The connection between natural frequencies and nodal diameters is shown via the SAFE (Singh's Advanced Frequency Evaluation) diagram in Fig. 5. The circles represent natural frequencies at maximum temperature and zero rotational speed, and the rectangles represents natural frequencies at minimum temperature and maximum rotational speed. Real natural frequencies lie between those borders. The lines between the natural frequencies are used only for a better visualisation. The dashed vertical lines represent the most excitable modes of the blisk (shape of vector of operating excitation and modal shape are equal)—in this case, the 13th nodal diameter (standing wave) and the 11th nodal diameter (travelling wave, second harmonics order).

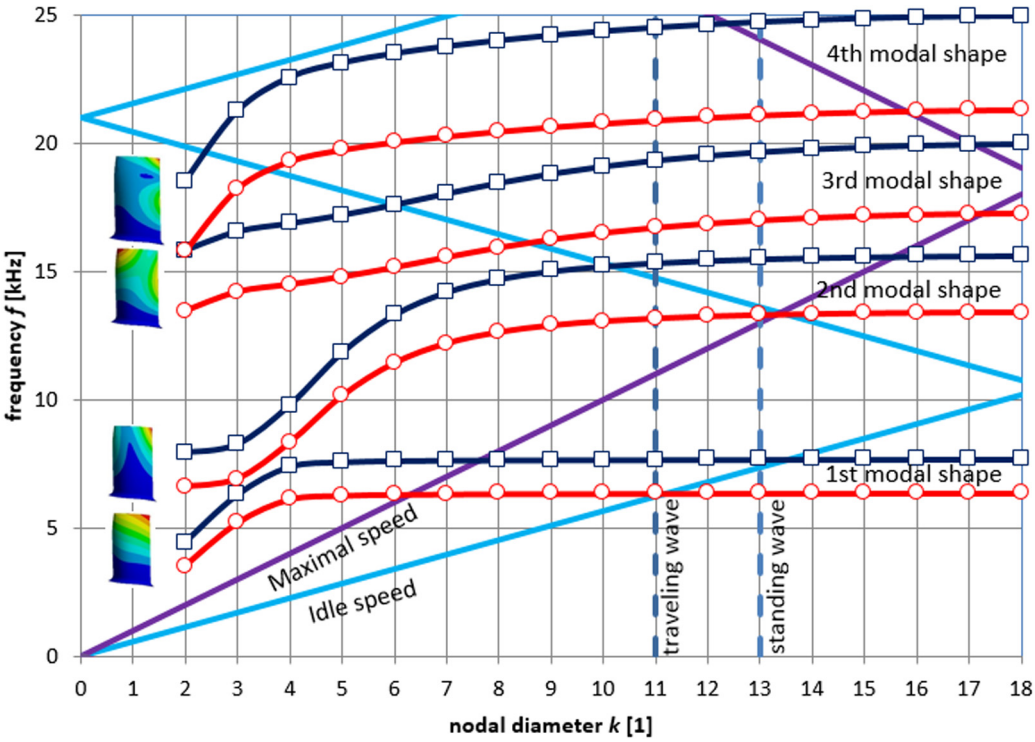

Fig. 5. SAFE diagram with the effect of temperature and centrifugal forces

4. Experimental modal analysis of the blisk

The natural frequencies of the blisk were determined by the experimental modal analysis (EMA) in Aerospace Technology Division testing station. The measuring system contained an impact hammer and microphone. The signal analyser recorded the measured amplitude-frequency characteristics of individual blades (the others being properly damped). This method of measurement of natural frequencies was tested on an impeller wheel and were in very good agreement with the results of computational modal analysis. Measured mistuning of individual impeller blades was almost zero.

On the basis of modal tests, it was found that the blades of blisk are highly mistuned up to 130 Hz in the case of the first bending mode, which is in the operating speed area, provided by the first harmonic of 13 vanes, a difference of up to $600\,\mathrm{min}^{-1}$. The mistuning of the blisk blades leads to very serious consequences. Due to its influence, nodal diameters do not rotate any longer. The blades vibrate according to the shape of mistuning, where the individual nodal diameters do not move and the most mistuned blade or blades accumulate the energy supplied by the other blades, [6].

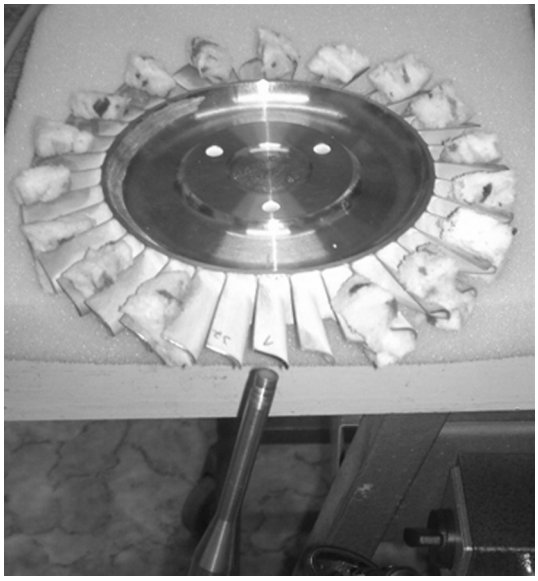

Fig. 6. Measuring system and the blisk with damped blades

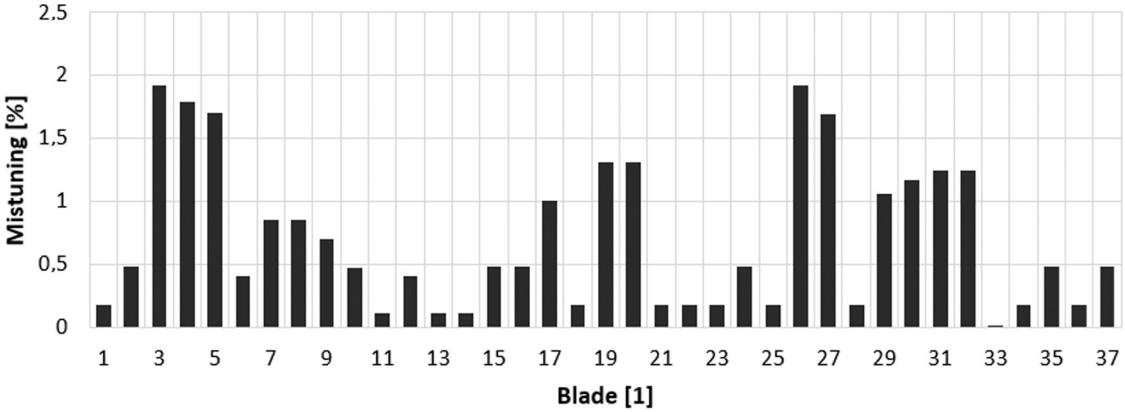

Fig. 7. Mistuning of blades

The average value of the measured natural frequencies $\bar{f}_i$ was very similar to the calculated natural frequencies (blisk with the maximum possible number of nodal diameters), see Table 2. The natural frequencies of the four blisks were not too different from each other, except for the first torsional shape. For mass production, it is desirable to have the effect of blade mistuning minimised, thereby reducing the critical speed to a minimum and avoiding failure.

Table 2. Deviation between experimental and computational modal analyses

Mode/ Blisk	**EMA vs FEM deviation [%]**			
	f_1	f_2	f_3	f_4
1	1.64	0.06	0.78	0.85
2	1.80	1.04	0.90	0.02
3	1.25	0.60	0.99	0.34
4	1.45	0.23	0.46	0.07
$\bar{f}_i$	1.54	0.48	0.78	0.32

5. Methodology of the vibration tests

Due to the absence of an advanced telemetry monitoring device, which would allow measurement of real stress level during operating at high temperature and rotating speed, a new simple vibration test methodology was developed. The required process of the vibration test, valid for any rotational speed area, is clearly shown in Fig. 8. One cycle represents the first ramp to the upper speed limit or a drop to the lower one. Each cycle contains one overpass of desired speed during which all blades are excited.

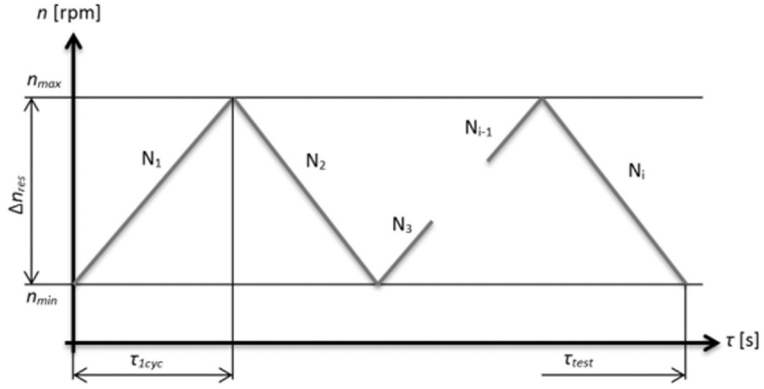

Fig. 8. Scheme of the vibration test program

The number of cycles representing an unlimited life was determined to be $N_f = 1 \cdot 10^7$. Assuming the width of the resonance zone Δf_{res} (considering the influence of mistuning and damping) and the desired cycle length $\tau_{1\mathrm{cyc}} = 90$ minutes (one acceleration or deceleration therefore takes 1.5 hours), the increase of speed Δa, rate of change of excitation speed ΔA and finally the resonance wide Δn_{res} in the rotational speed domain and width testing area Δn was determined

$$\Delta a = \frac{\Delta n}{\Delta \tau_{1\mathrm{cyc}}}, \tag{4}$$

$$\Delta A = \frac{\Delta f}{\Delta \tau_{1\mathrm{cyc}}}, \tag{5}$$

$$\Delta n_{\mathrm{res}} = \frac{\Delta f_{\mathrm{res}}}{h \cdot s}. \tag{6}$$

To achieve $N_{\mathrm{HCF}} = 1 \cdot 10^7$ cycles (the expected level HCF – High-Cycle Fatigue) with consideration of calculated resonant frequencies $\bar{f}$ (mean frequency in the tested range of rotational speeds), life at this frequency in particular areas is guaranteed for a total of approximately τ_{HCF}

$$\tau_{\mathrm{HCF}} = \frac{N_{\mathrm{HCF}}}{\bar{f}}. \tag{7}$$

The time spent on the resonant frequency during one cycle (acceleration or deceleration) is

$$\tau_{\mathrm{res}} = \frac{\Delta n_{\mathrm{res}}}{\Delta a}. \tag{8}$$

The minimum number of cycles N_i needed (1 cycle = ramp or fall on the upper or lower speed limit) to achieve the time spent on the resonant frequency τ_{HCF} is determined on the basis of

the calculated time spent on resonance τ_{res} (assuming the size of the resonant peak Δf_{res}). The number of test cycles iss rounded to even numbers upwards

$$N = \frac{\tau_{\mathrm{HCF}}}{\tau_{\mathrm{res}}}. \tag{9}$$

The total test time for one rotational speed area is

$$\tau_{\mathrm{test}} = N \cdot \tau_{1\mathrm{cyc}}. \tag{10}$$

Four ranges of rotational speed for the vibration test were scheduled. Two of them for the excitation of 1st and 2nd natural frequencies by the first harmonic order, and another two for the 3rd and 4th natural frequencies excited by the second harmonic of the engine excitation order.

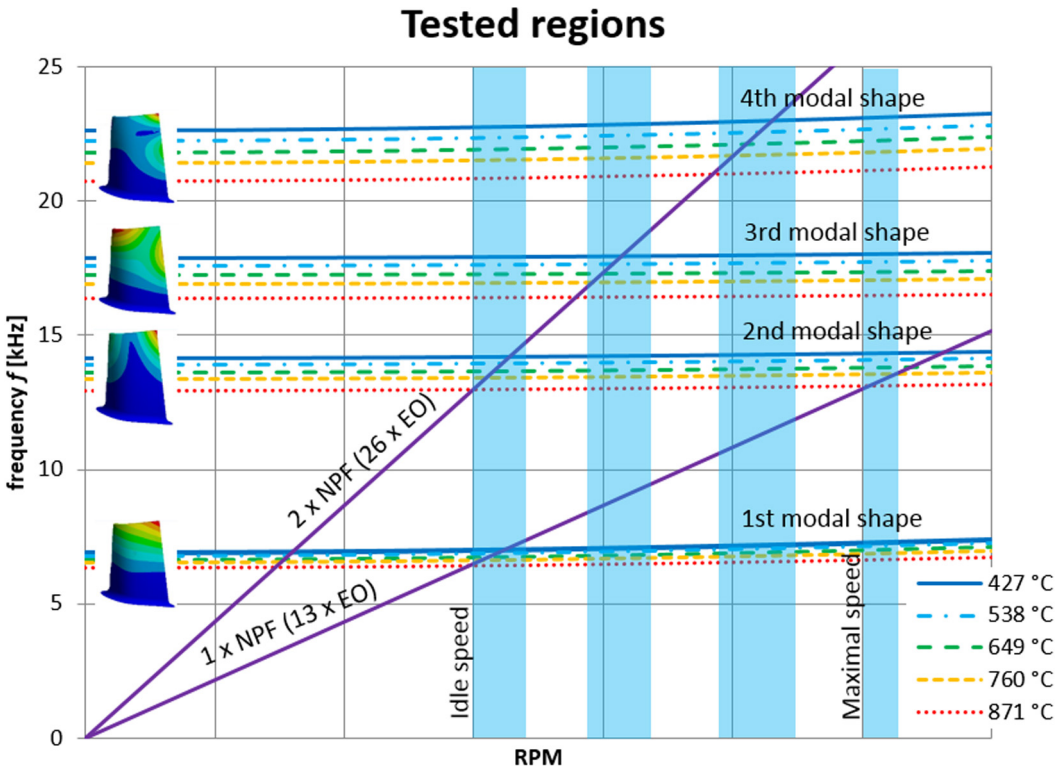

Fig. 9. Experimental regions for the verification of rotational speeds

6. Result of vibration test

Using the vibration tests on four blisks, we identified the first critical speed, which lies in the performance interval of $2 \div 5$ % above the idle speed.

To limit the number of passes through the critical speed during acceleration to the operating speed, the idle speed was newly shifted to 8 % above the idle speed, which should be a sufficient margin against resonance and for the frequency mistuning of the individual blades. During the search for the first natural frequency, two blisks were destroyed because the high cycle life limit was reached, see the crack in Fig. 10. In other cases, cracks initiations indicating HCF were searched for by the very sensitive Fluorescent Penetration Inspection (FPI).

The maximum operating speed was located below the second natural frequency excited from the first harmonic order of 13 stator vanes and thus it would reach a standard engine operation

Fig. 10. Crack surface on the blade root

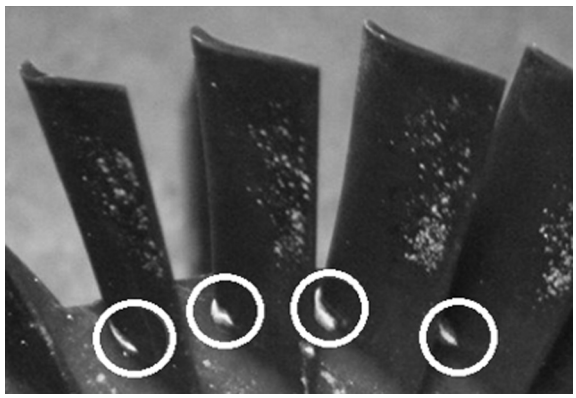

Fig. 11. Indication of HCF (highlighted) found by using fluorescent penetration inspection

range. During the vibration tests, the range of the maximum operating speed was verified on three blisks (before the destruction of two of them in the previous case).

Furthermore, it was found that the influence of the second harmonic order of the 13 vanes is irrelevant (no initiations were found) and does not need a quick pass through acceleration to achieve the operating speed. It was also found that the experimental results matched the numerical analysis of the blisk natural frequencies for a selected number of nodal diameters. In the case of modal analysis of the blisks, it is necessary to consider their changing frequency depending on the rotational speed and temperature. Information about the actual temperature profile along the disc-blade system has not yet been obtained with such precision that can be used to sufficiently narrow natural frequency ranges in Campbell diagrams, and thus it was not possible to obtain a closer estimated position of the critical (resonant) rotational speed.

After each vibration test the EMA (steady non-rotating state of the blisk at room temperature) was carried out, the natural frequency of blades of specific blisks was not changed (differences were probably caused by the error of measurements).

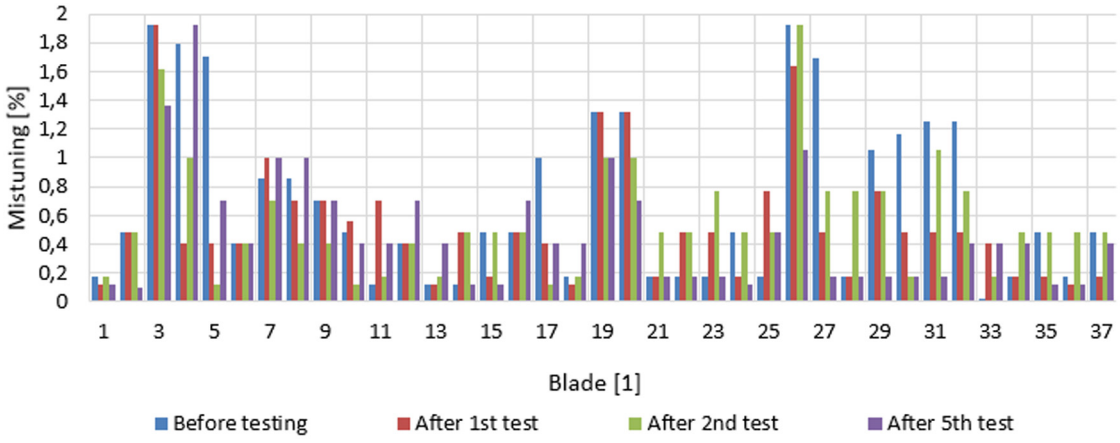

Fig. 12. Natural frequencies during testing

In the next phase of testing, the performance range of $2 \div 5$ % above the idle speed was forbidden by the control unit and idle speed was shifted to the 2 % under the idle speed. After more than 4 000 quick overcomes (or starts) of this area, a crack indication at one blade was found. The value represents life in terms of high-cycle fatigue.

7. Conclusion

The subject of this paper is a clear summary of all achievements of computational modelling and testing of new turbine stage for turbojet engine, implemented at the Department of Engineering Analyses and testing station of DLT of První brněnská strojírna Velká Bíteš.

For a new proposal of turbine stage with 13 vanes and 37 rotor blades, a vibration test was developed to verify HCF durability and localization of possible resonant areas in the operating speed range. A good agreement between the experimental results and the numerical computation of natural frequencies of the blisk was found. Resonance frequencies were located in the operating speed performance range of $2 \div 4$ % above the idle speed. For an additional operation of new turbine stage, this range of rotational speed was not permitted. The idle speed was increased to the value of 8 % above the original idle speed. High mistuning of blades within the blisk was also revealed, which was probably caused by the lost wax method. The mistuning of blades up to 200 Hz had a negative effect on the width of resonance frequencies.

The acquired knowledge should also serve to propose new turbine stages and optimise the time required for the implementation of vibration tests to verify HCF resistance of newly designed blisks. The new design of blisk was approved for production, because no danger of resonance was found.

Acknowledgements

This work was supported by Aerospace Technology Division of První brněnská strojírna Velká Bíteš, a. s.

Reference

[1] Bertini, L., Monelli, B. D., Neri, P., Santus, C., Guglielmo, A., Explanation and application of the SAFE diagram, Proceedings of the 11$^{\text{th}}$ International Conference RASD 2013, Pisa, Italy, pp. 1–15.

[2] Doležal, Z., Excitability of coupled vibration of an radial compressors impellers, VZLÚ, Prague, 1987. (in Czech)

[3] Kushner, F., Disc vibration-rotating blade and stationary vane interaction, Journal of Mechanical Design 102(3) (1980) 579–584.

[4] Kushner, F., Disk resonance equations & interference diagrams, International Turbomachinery, June 2012.

[5] Kushner, F., Richard, S. J., Strickland, R. A., Critical review of compressor impeller vibration parameters for failure prevention, Proceedings of the 29th Turbomachinery Symposium, Turbomachinery Laboratory, Texas A&M University, College Station, Texas, 2000, pp. 103–112.

[6] Sheng, X., Clay, D. C., Allport, J., Dynamics of mistuned radial turbine wheel, Proceedings of the 8$^{\text{th}}$ International Conference on Turbochargers and Turbocharging, London, UK, 2006.

[7] Sheng, X., Model identification and order response prediction for bladed wheel, Journal of Sound and Vibration 323(1-2) (2009) 194–213.

[8] Statečný, J., Doležal, Z., Strength and durability of aircraft turbine engines, Part II, Prague, 1991. (in Czech)